1.3.5 Fluorescent proteins and their chromophore analogues: photophysics and biosensing

*The complex photophysics of fluorescent proteins (FPs) in conjunction with advanced spectroscopic and microscopic techniques makes it possible to map several biochemical parameters (*e.g. *pH and concentration of ions) at submicrometric resolution. Furthermore 3D imaging of living cells within intact tissues, organs, and whole animals, is accessible through multiphoton excitation. Here we report our results on the photophysics of photoactivation/deactivation of some FPs and of their synthetic chromophore analogues. We exploites this knowledge for nano-resolution imaging and for the development of new reversibly-switchable FP mutants. Finally, we report our findings on FP multiphoton excitation spectra, in particular in light of the implementation of FP-based sensors for pH and chloride suitable for in vivo applications.*

Photoswitching and cis-trans photoisomerization

Novel imaging techniques emerged in recent times thanks to the development of new FPs that can be reversibly or irreversibly photoconverted between two optical states that added a "temporal dimension" to imaging of proteins at intracellular level also *in vivo*. The most impressive results were obtained by using *reversibly* switchable FPs (RSFPs) [1-4], as they allow repeated activation events, thus prolonging the observation of biological dynamics, and the photo-labeling of several subcellular regions one after the other. Furthermore, RSFPs stand as excellent fluorophores for novel nano-resolution imaging techniques based on the regioselective activation/deactivation of emissive states at the nanoscale.

We linked the photoswitching behavior of certain FPs to chromophore *cis-trans* photoisomerization. We investigated also the spectral and structural modification of synthetic chromophore analogues upon irradiation, and determined for the first time the optical, NMR and Raman spectra of neutral *trans* isomers (Fig. 1), along with photoconversion quantum yields φ_c. Surprisingly, φ_c ranges from 0.1 to 1.0, demonstrating that photoconversion is a general and very efficient intrinsic photophysical mechanism of FP chromophores, whose efficiency is modulated by the mutant-specific protein environment [1,4]. Starting from these results, we developed butenolide derivatives structurally related to the GFP chromophore; we examined in detail the photophysics of these structures, with particular attention paid to their solvatochromic and photoswitching behavior [5,6]. Butenolide derivatives show ratiometric read-out of their fluorescence emission related to polarity of the environment, and fluorescence emission related to its dielectric constant; their straightforward engineering in bio-derivatized structures for membrane and intracellular targeting and their scarce cytotoxicity were exploited in the measurement of dielectric constant in different subcellular domains (Fig. 2) [6].
Pre-resonant Raman experiments are able to determine the vibrational features of the chromophore also when embedded in the proteins (Fig. 1g,h). We studied the Raman signatures of different chromophore states in GFP mutants and compared them to those of the isolated chromophores. Our experiments allowed us to demonstrate that the *cis-trans* isomerization is responsible for the photoswitching behaviour of at least two RSFPs, namely EYQ1 (a newly developed GFP variant with T203Y E222Q) and BFPF (Y66F) [4]. In particular,

for the case of EYQ1 we showed that at pH=8 the chromophore is anionic in the native form and neutral *trans* in the photoconverted form; it is neutral *cis* in the native form at lower pH. Our investigation highlights the relevance of Raman spectroscopy for the study of the ground and metastable states of optically-active portions of proteins.

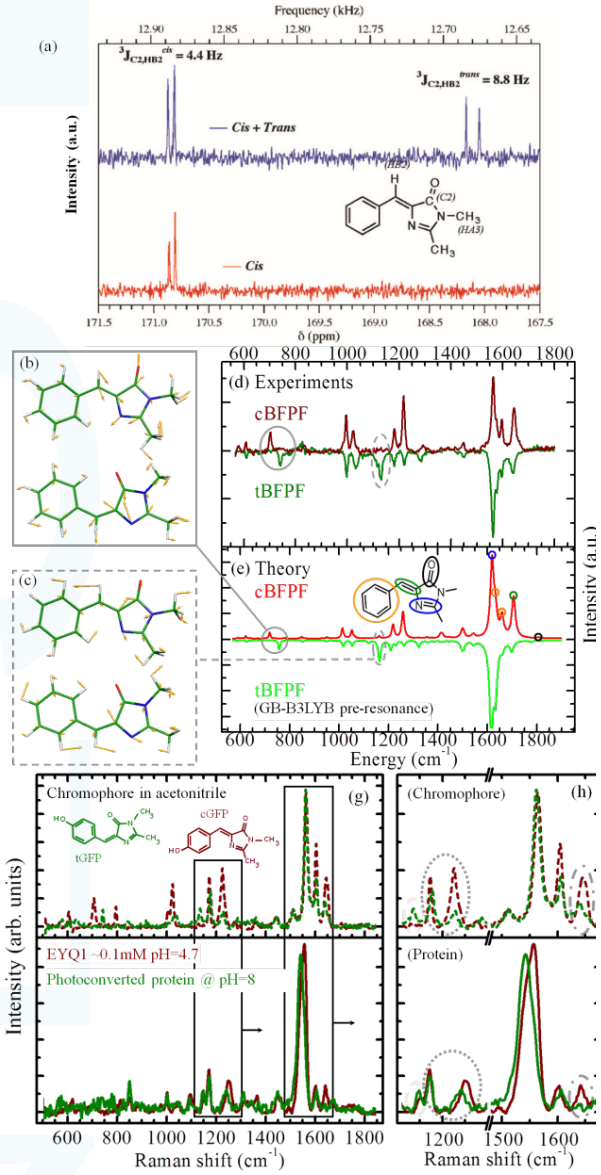

Figure 1. (a) ^{13}C-NMR spectra of native and photoconverted cBFPF while adopting selective decoupling between the methyl protons HA3 and C2: the detected $^{3}J_{C2,HB2}$ values in the photoproduct correspond to those expected for the *cis* and *trans* isomers. MIDDLE: Experimental (d) and calculated in vacuo (e) pre-resonant Raman spectra of the isolated chromophore of BFPF in *cis* and *trans* forms (cBFPF, tBFPF); the spectra of the photoconverted form are shown inverted around the x-axis. Solid and dashed gray ellipses highlight two of the modes that change significantly in the cis-trans transition, and that are described in panels (b) and (c). Small circles emphasize stretching modes localized on double bonds in the chromophore region, highlighted in the inset of panel (e) with corresponding color: black, C=O; green, C=C on the bridge; orange, C=C on the phenylic ring; blue, C=N. BOTTOM: The dark red solid curves represent the Raman spectrum of native EYQ1 at pH=4.7 after the subtraction of the baseline, and the dark green solid curves represent the spectrum of the photoconverted form at pH=8. For comparison are reported the Raman spectra of its neutral chromophores in *cis* and *trans* forms (cGFP and tGFP, dark red and dark green dashed curves, respectively). Panel (g) contains magnifications of the highlighted regions in panel (h); the ellipses emphasize peaks with similar behavior for isolated and protein-embedded chromophores

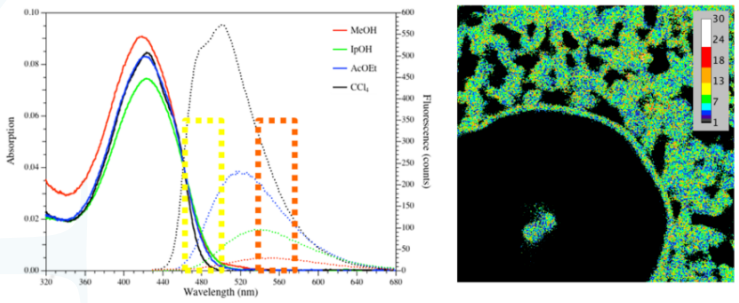

Figure 2. LEFT: absorption and fluorescence emission spectra of a butenolide derivative. The two channels selected for ratiometric analysis are highlited. RIGHT: dielectric constant map of butenolide dye in living cell.

In order to develop more efficient RSFPs, we focused on residues adjacent to the chromophore that can hinder this "intrinsic" photochromic behaviour. Hybrid QM/MM methods were applied to FPs to understand their structure/function relationship, i.e. how different chromophore structures and the amino acids surrounding the chromophore tune the excitation/emission spectrum [7]. Also with the help of these computational studies, we demonstrated that the E222Q replacement induces reversible photoswitching in four GFPs otherwise differing in the mutation pattern, and yields switching 2-3 orders of magnitude faster than in any other previously reported photoswitchable GFP [2,3]. We assessed the utility of the new RSFPs for intracellular studies *e.g.* by inverse Fluorescence Recovery After Photobleaching (iFRAP), a technique that relies on the localized photoactivation of a fluorophore and the real-time monitoring of its subsequent dynamics. EYQ2 (S65T/T203Y/E222Q) was conjugated to a short peptide sequence that acts as a nuclear localization signal (NLS), *i.e.* it is recognized by the cellular importin system and actively transported to the nucleus. Then, the dynamics of the nucleocytoplasmic shuttling of NLS-EYQ2 was determined by iFRAP (Fig. 3d). EYQ2 allowed for the long-term repetition of the experiment in the same cell, thus increasing the accuracy of kinetic measurements and ideally providing the correlation of transport dynamics with different cell states. iFRAP on NLS-EYQ2 yielded a shuttling time-constant (t=117±3 s) in excellent agreement with the value measured by conventional FRAP on NLS-EGFP.

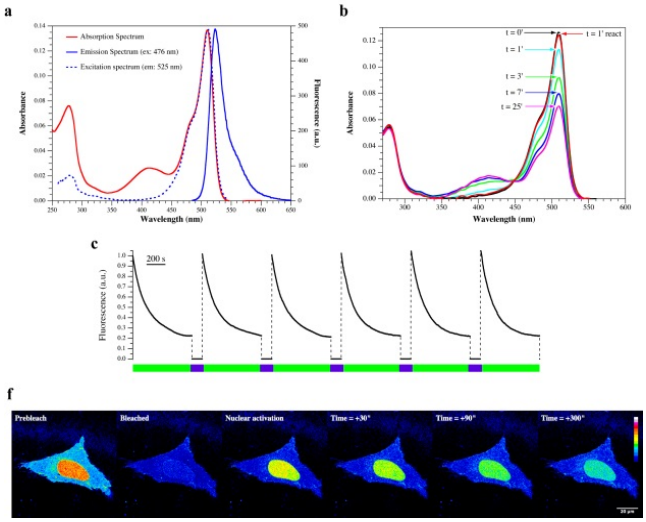

Figure 3. (a) Absorption (red line), emission (solid blue line), and excitation (dashed blue line) of EYQ1 (T203Y/E222Q) at pH 7.2; (b) Absorption spectrum photoconversion of EYQ1 at pH 8.7: following 514 nm-illumination (0.5 W/cm^2) the anionic chromophore band (510 nm) decreases its intensity and the dark state band at 410 emerges (t=0' to 25'); 405 nm-illumination (0.06 W/cm^2) for 1' is sufficient to restore the original absorption (t=1' react); (c) photoswiching on/off cycles of EYQ1 in transfected HeLa cells by means of 514-nm (*bleaching cycle: green*) and 403-nm (*reactivation step: violet*) laser light; (d) iFRAP of NLS-EYQ2 in one HeLa cell: initially fluorescence is bleached off cell-wide by 514 nm scan-irradiation; then, fluorescence is reactivated only in the nucleus by means of short (1s) 405-nm point-irradiation and the cell is imaged by using low power 514 scan-excitation

pH/chloride biosensing

The chromophore of E^{n}GFP can exist into two optically-distinguishable forms

(neutral and anionic) that are both fluorescent; such a dual fluorescence property makes possible the fabrication of ratiometric (i.e. concentration independent) pH sensors tailored to the 5-9 pH range [8,9]. Moreover, the S65T mutation introduces a specific anion-binding site in E^nGFP [8,10]. We thus decided to exploit this peculiarity in the development of a novel chloride sensor. Monitoring these parameters is of much relevance: pH is a remarkable modulator of cell structure and function, and Cl^- participates in many physiological functions including stabilization of neuronal resting potential, charge balance in vesicular acidification, and regulation of cell volume. Our sensor was conceived as ratiometric, genetically-encoded and capable to simultaneously measure [Cl^-] and pH. To this end, a monomeric red protein insensitive to chloride and pH (DsRed) was fused to E^2GFP via a peptide linker, creating the sensor called Clophensor in Fig. 4 [10]. In vitro and results in living cells demonstrated the functionality of the sensor in the physiological range of pH and for Cl^- concentration ranging from 300mM down to less than 1 mM.

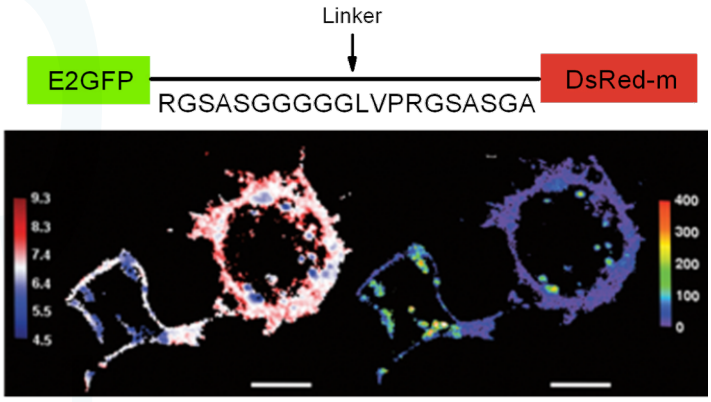

Figure 4. TOP: Cartoon scheme of the ClopHensor: E2GFP is the pH and Cl^- sensing portion, DsRed-m is the reference portion of the sensor; BOTTOM: pH (left) and [Cl^-] (right) maps in living hek293 cells. The sensor was targeted to the membrane and to large dense core vesicles by means of suitable labeling (gap43 and neuropeptide Y, respectively). White bar: 5μm

We are pursuing the use of this biosensor in deep-tissue mapping, aiming at *in-vivo* experiment that can be performed via two-photon excitation microscopy. To this end, two-photon excitation and photoconversion spectra have been measured [8] and, in view of actual invio applications, an *in-utero* electroporation technique was demonstrated to control the localization for the expression of exogenous proteins in the brain of living mice [11].

From a computational point of view, we investigated the two-photon absorption (TPA) properties of various fluorescent proteins (BFP, CFP, GFP, DsRed, mOrange, zFP and Kaede), and compared them with one-photon properties, using computational methods based on Density Functional Theory. This technique allowed us to calculate excitation wavelengths and cross sections for various model chromophores. A general relationship between excitation wavelength and structure was extracted, based on the variation of electric dipole upon excitation, and ultimately connected with the extension of the π-conjugated system (an example in Fig. 5b) [7]. The two-photon calculations shed light on the peculiar TPA features of DsRed (Fig. 5a), and predicted the presence of high-energy (500-700 nm) TPA bands in several other FPs. These excitation bands, later confirmed by experiments, can provide researchers with useful, and yet unexploited, spectral windows for two-photon imaging.

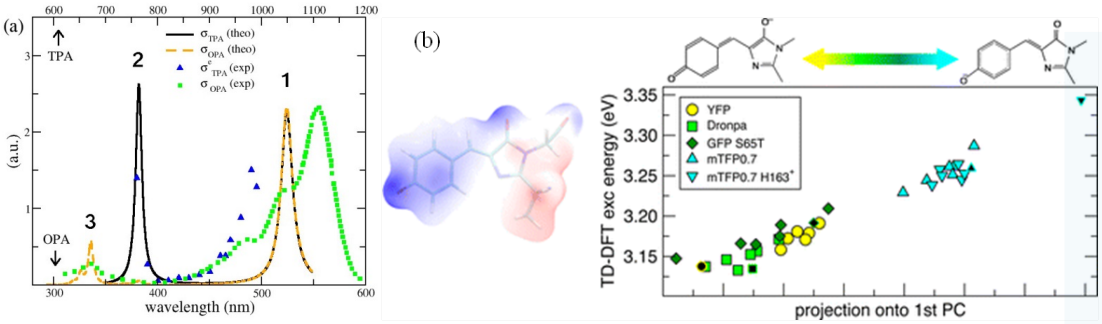

Figure 5. (a) Comparison between experimental and theoretical spectra of DsRed. The two-photon measured cross section (blue triangles) displays a strong increase below 800 nm (band **2**), whereas the one photon spectrum (green squares) is rather featureless in that region. The calculated TPA cross section (black solid line) reproduces this band, as due to excitation at a higher excited state. The blue shift between the theoretical and experimental **1** band is due to having considered the isolated model chromophore instead of the entire protein, to intrinsic errors of the theory, and to neglect of vibronic features. (b) Left: Electrostatic potential of the surrounding protein matrix mapped onto the chromophore molecular surface. Right: QM/MM TD-DFT excitation energy as a function of chromophore structure (described by a suitable linear combination of bond lengths) for various FP structures.

References

[1] Cis-trans photoisomerization of fluorescent-protein chromophores. J. Phys. Chem. B **112**, 10714 (2008). V. Voliani, R. Bizzarri, R. Nifosì, S. Abbruzzetti, E. Grandi, C, Viappiani, and F. Beltram

[2] Photoswitching of E222Q GFP mutants: "concerted" mechanism of chromophore isomerization and protonation, Photochem Photobiol. Sci. **9**, 1307 (2010). S. Abbruzzetti, R. Bizzarri, S. Luin, R. Nifosì, B. Storti, C. Viappiani, F. Beltram.

[3] Single aminoacid replacement makes Aequorea Victoria fluorescent proteins reversibly photoswitchable, J. Am. Chem. Soc. **132**, 85 (2010). R. Bizzarri, M. Serresi, F. Cardarelli, S. Abbruzzetti, B. Campanini, C. Viappiani, F. Beltram.

[4] Raman Study of Chromophore States in Photochromic Fluorescent Proteins. J. Am. Chem. Soc. **131**, 96 (2009). S. Luin, V. Voliani, G. Lanza, R. Bizzarri, R. Nifosì, P. Amat, V. Tozzini, M. Serresi, F. Beltram.

[5] Cis–trans photoisomerization properties of GFP chromophore analogs, Eur Biophys J. **40**, 1205 (2011). G. Abbandonato, G. Signore, R. Nifosì, V. Voliani, R. Bizzarri, F. Beltram.

[6] Imaging the static dielectric constant in vitro and in living cells by a bioconjugable GFP chromophore analog, Chem. Commun. **49**, 1723 (2013). G. Signore, G. Abbandonato, B. Storti, M. Stockl, V. Subramaniam, R. Bizzarri.

[7] Spectral "fine" tuning in fluorescent proteins: the case of the gfp-like chromophore in the anionic protonation state, J Chem Theory Comput **9**, 497 (2013), P. Amat, R. Nifosì.

[8] Green Fluorescent Protein-based pH indicators for in vivo use: a review, Anal. Bioanal. Chem. 393, 1107 (2009). R. Bizzarri, M. Serresi, S. Luin, F. Beltram.

[9] Real-time measurement of endosomal acidification by a novel genetically encoded biosensor, Anal. Bioanal. Chem. **393**, 1123 (2009). M. Serresi, R. Bizzarri, F. Cardarelli, and F. Beltram.

[10] Simultaneous intracellular chloride and pH measurements using a GFP-based sensor, Nature Methods **7**, 516 (2010). D. Arosio, F. Ricci, L. Marchetti, R. Gualdani, L. Albertazzi, F. Beltram.

[11] High-performance and site-directed in utero electroporation by a triple-electrode probe, Nat Commun. **3**, 960 (2012). M. dal Maschio, D. Ghezzi, G. Bony, A. Alabastri, G. Deidda, M. Brondi, S. Sulis Sato, R.P. Zaccaria, E. Di Fabrizio, G.M. Ratto, L. Cancedda.